Structure-Property Correlation Studies of Nitrogen donor Ligand based Metal–Organic Framework

A Thesis submitted to
Indian Institute of Science Education and Research, Pune
In partial fulfilment of the requirements for the
MS Programme

Thesis Supervisor: Dr. Sujit K. Ghosh (IISER Pune)

By
Shweta Singh
Registration No. 20081018
Chemistry Department
April, 2014

Indian Institute of Science Education and Research Pune,
900, NCL Innovation Park, Dr Homi Bhabha Road Pune, Maharashtra 411008, India

CERTIFICATE

This is to certify that this dissertation entitled "**Structure-Property Correlation Studies of Nitrogen donor Ligand based Metal–Organic Framework**" towards the partial fulfilment of the MS programme at the Indian Institute of Science Education and Research, Pune represents original research carried out by Shweta Singh at IISER Pune under the supervision of Dr. Sujit K. Ghosh, Assistant Professor, Department of Chemistry during the academic year 2013-2014.

Signature of student

Date

Signature of supervisor

Date

DECLARATION

I hereby declare that the matter embodied in the report entitled "**Structure-Property Correlation Studies of Nitrogen donor Ligand based Metal–Organic Framework**" are the results of the investigations carried out by me at the Department of Chemistry, IISER Pune, under the supervision of Dr. Sujit K. Ghosh and the same has not been submitted elsewhere for any other degree.

ACKNOWLEDGMENT

Foremost, I would like to express my sincere gratitude to my mentor Dr. Sujit K. Ghosh for the continuous support offered throughout the tenure of the project. His mentorship was paramount in providing a well-rounded experience consistent my long-term career goals.

Besides my advisor, I would like to thank the rest of my thesis advisory committee for encouragement and insightful comments.

My sincere thanks also goes to my co-guide Biplab Manna for his patience, motivation, enthusiasm and immense knowledge. His guidance helped me in all the time of research and writing of this thesis.

I thank my fellow lab mates: Sanjog Nagarkar, Biplab Joarder, Soumya Mukherjee, Avishek Karmakar, Aamod Desai, Partha Samanta and Amrit Kumar for the stimulating discussions and for all the fun we had in the last couple of years.

Last but not the least; I would like to thank my family for all the love, assistance and guidance they have provided me throughout my life.

ABSTRACT

Ligand **L** (L= 1, 4-bis (4-pyridyl)-2, 3-diaza-1, 3-butadiene) belonging to an interesting family of nitrogen-donors has been utilised with Cd(II) salt in constructing two 2D MOFs. Crystallographic characterisations reveal that the two polymeric frameworks contain counter anions which are coordinated to the metal centres. Through a novel anion exchange process, the coordinated anions can be exchanged without destructing the framework. Both the compounds undergo structural changes upon replacement of the coordinated anions by foreign anions, which is evident from the slight variations in the PXRD patterns with respect to the corresponding parent compounds. Such phenomenon gives an indication of dynamism in the framework. This anion exchange process is highly selective, N_3^- being the most preferred by the framework. Interestingly, both the compounds exhibit anion-responsive tunable luminescence.

TABLE OF CONTENTS

LIST OF FIGURES

INTRODUCTION

Over the past five decades, lots of analysis has been done on porous materials, seeking widespread applications in each biological and industrial process. Zeolites which are porous aluminosilicates are one amongst the abundant glorious examples.[1] Such porous materials permit guest molecules to diffuse into the bulk structure, and therefore the form and size of the pores ends up in shape- and size-selectivity over the guests which can be incorporated. Once incorporated, chemical transformations of the guests might happen.

Later, a couple of research groups found out the probabilities for brand spanking new material structures and properties offered by coordination polymers. In theory, the wide selection of metal, and also the infinite choice and design of ligands, displays a broad spectrum of structural, magnetic, electrical, optical, and chemical change properties that such materials exhibit.

Metal-organic frameworks [2] (MOF) or Porous Co-ordination Polymers (PCP) are a very recent category of nanoporous polymeric material, consisting of clusters of metal ions held together in a three-dimensional space by organic bridging ligands. These materials are a new development on the interface between molecular coordination chemistry and materials science. A wide range of novel structures have been prepared which feature amongst the largest pores noted for crystalline

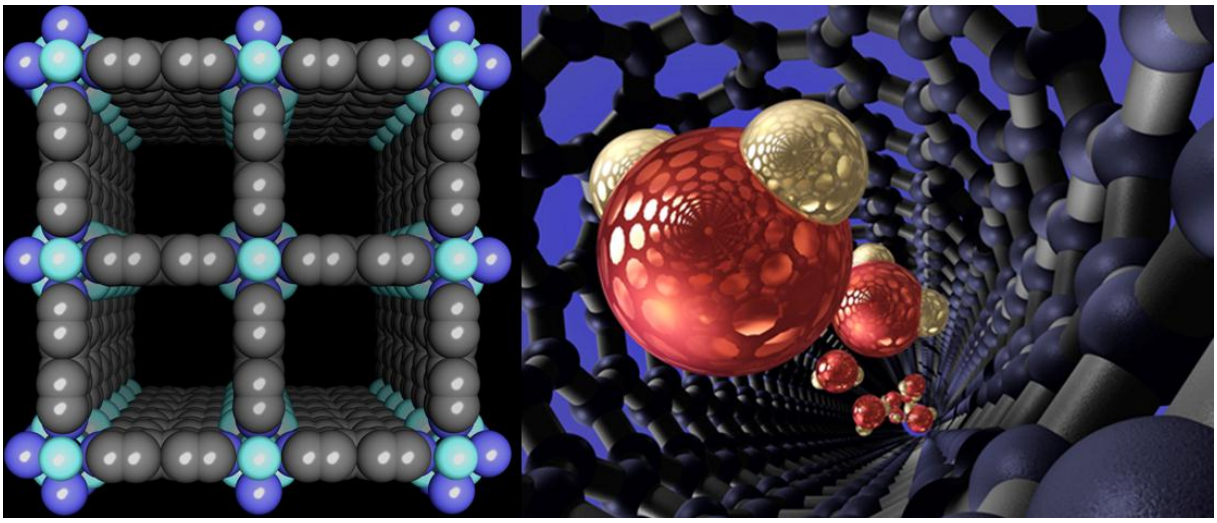

Figure 1: A 3D porous MOF [14] (left) and selective sorption of guest into the pores of a MOF (right) [15]

compounds with terribly high sorption capacities not seen in zeolites. Varied uses are investigated, including gas storage/separations [3], non-liner optics [4], molecule recognition [5], and catalysis [6].

Porous coordination polymers are usually classified into three distinct categories- first, second and third generations (*Figure 2*). The first types are the ones with no permanent porosity i.e. the framework is known to collapse irreversibly after the removal of the guest molecule. The second generation materials possess a stable and robust structure which remains unaltered both before and after guest sorption. The third of the kind are the foremost attention-grabbing of all as they show structural dynamism [7]. In simpler terms, this suggests that these compounds are versatile. They are flexible and they reversibly respond to the stimuli, not solely chemical, however conjointly physical.

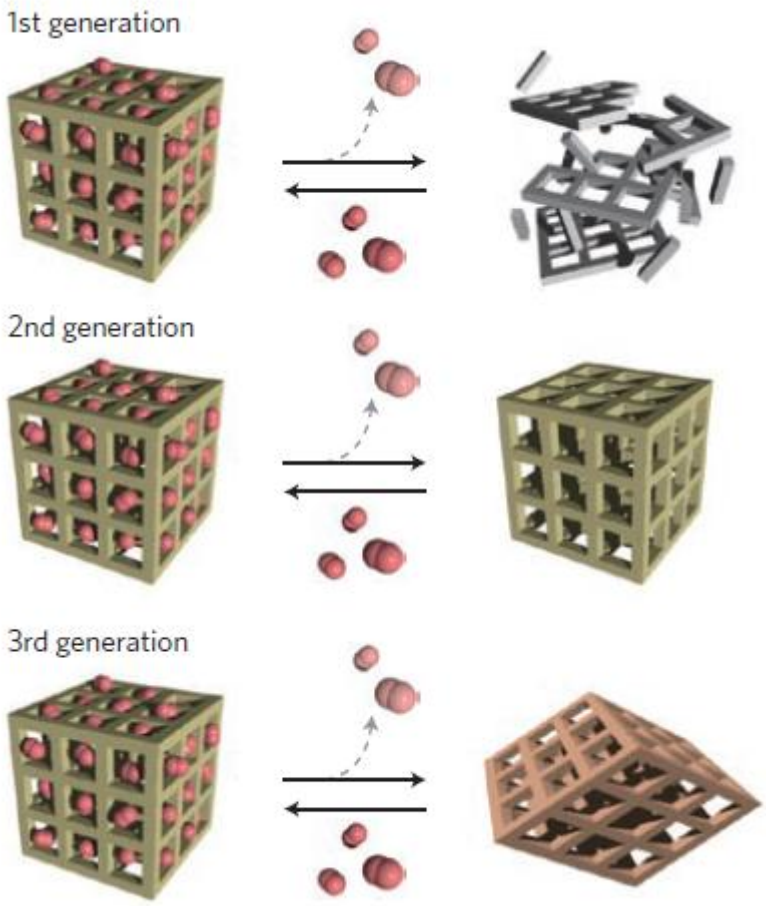

Figure 2: Classification of porous coordination polymers into three categories[7]

In the recent years, a number of research groups together with the acknowledged ones have dug into the third generation materials and have reported their significance over the rigid frameworks. The guest dependent dynamism of such compounds has caught immense attention. Such materials are very sensitive to the chemical environment; they undergo structural changes upon guest inclusion. Amongst the various MOFs reported so far, cationic MOFs (*Figure 3*) have proved to be opportune over the others in rendering a framework dynamic [8]. They are predominately designed by combining neutral ligands with metal ions, wherein the extra framework anions are either held in the framework voids or are weakly co-ordinated to the metal centre. These free anions are readily exchanged with a variety of anions of similar geometry to show

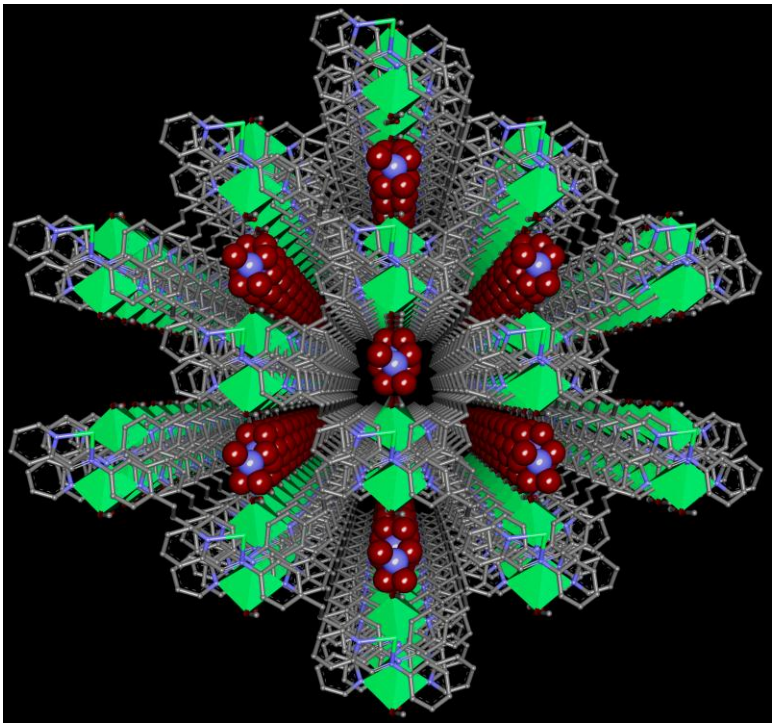

Figure 3: Cationic framework showing free anions in the channel[8]

interesting physical and chemical properties. These cationic MOFS have attracted much attention in the recent past owing to their aesthetically appealing structures and their eminently promising properties which make them suitable for applications as storage, recognition and delivery materials. Moreover, they display rich host–guest behaviour with a variety of counter-ions or solvent molecules in their giant central cavities [9].

This new type of organic–inorganic hybrid material is certainly very promising as a multifunctional luminescent material because both the inorganic and organic moieties can provide platforms to generate luminescence. MOFs have various modes for generating luminescence, including MLCT, LMCT, LLCT, MMCT, etc. Furthermore, some guest molecules/ anion within MOFs can also emit and/or induce luminescence (*Figure 4*). Such types of luminescent MOFs are useful for designing chemical sensors with optical signalling [10]. The feasible anion exchange behaviour of a cationic framework often provides a platform for sensing/ capturing of anions[11].

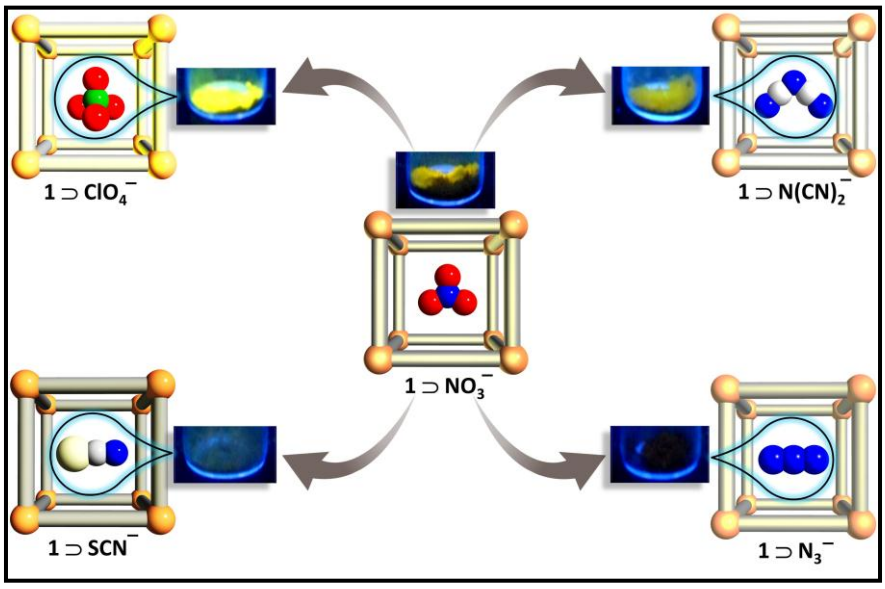

Figure 4: Diagrammatic representation of Anion responsive tunable luminescence [8]

Luminescent MOFs are very important because of their potential applications as sensors[12]. Selectivity and sensitivity of a MOF as chemical sensors can be enhanced by rendering dynamism to the framework [13]. Such a phenomenon is observed because of the guest responsive function of a dynamic MOF which eventually traps specific molecules.

It has been well reported that the structure of a MOF can be controlled by both ligand geometry and metal centre coordination. Therefore, inspired by the aforementioned progress in the study of these novel self-assembled structures, in this contribution, we here report the synthesis and characterisation of Cd(II) MOFs based on N-donor based ligand, **L**[16] (L= 1, 4-bis (4-pyridyl)-2, 3-diaza-1, 3-butadiene) which show interesting anion exchange behaviour and anion responsive luminescence.

EXPERIMENTAL SECTION

MATERIALS: All the reagents and solvents were commercially available and were used without further purification.

SYNTHESIS OF LIGAND L:

Scheme:

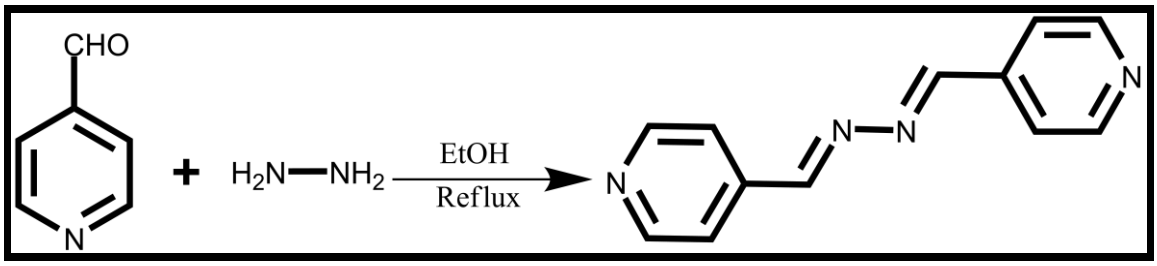

Procedure:

Schiff base condensation of 4-Pyridine carboxaldehyde (11.29 mL, 119.85 mmol) and hydrazine hydrate (3.65 mL, 59.92 mmol) in EtOH for about 24 hours at 70^{o}C gave rise to yellow crystalline compound. The product formed in the reaction was filtered off, washed with EtOH and dried over vacuum to yield the yellow coloured solid.

Calculated: For $C_{12}H_{10}N_4$: C 68.51, H 4.75 and N 26.75; *Found*: C 69.21, H 4.85 and N 25.95.

HRMS (ESI): *Calculated*: for $C_{12}H_{10}N_4$ $[M+H]^+$: 211.0983; *Found*: 211.0982.

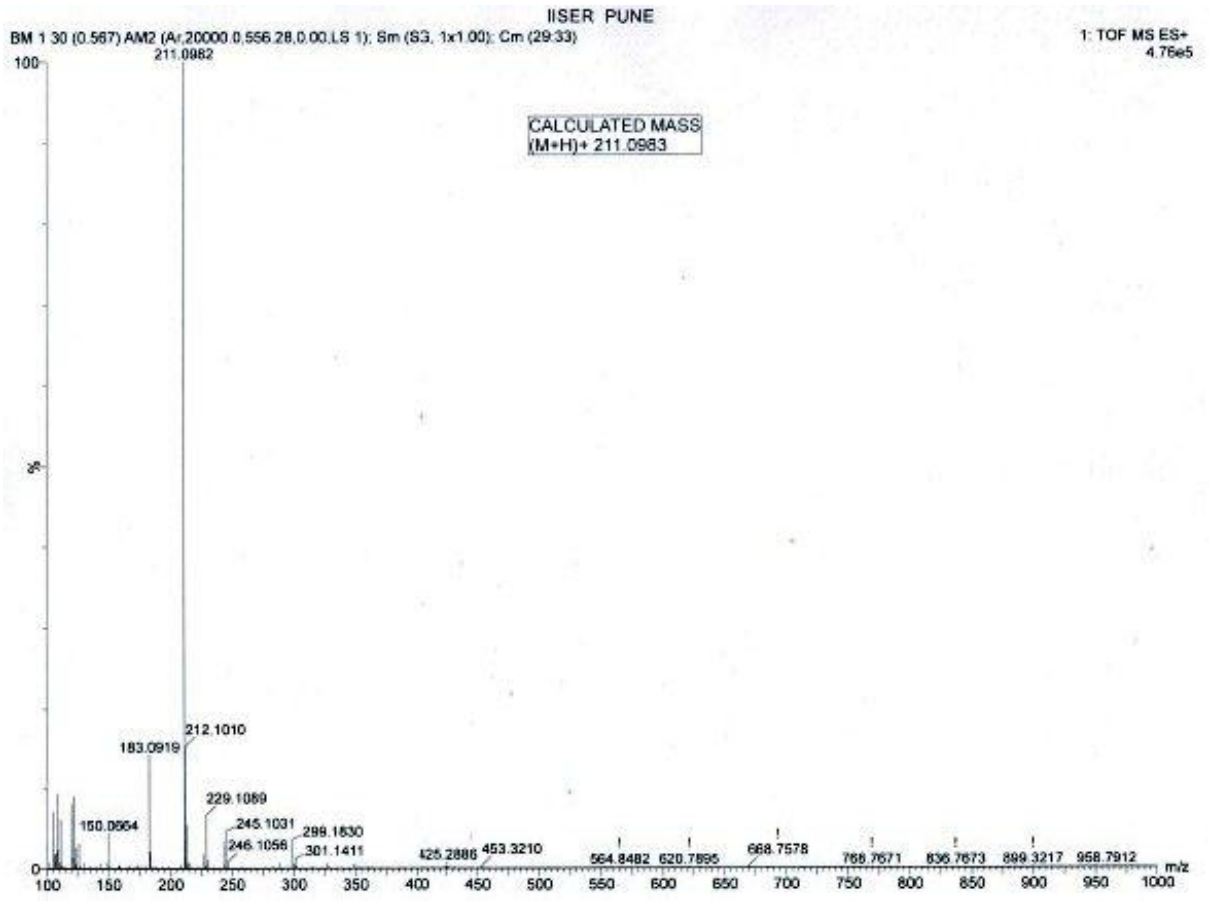

Figure 5: HRMS of Ligand L

SYNTHESIS OF COMPOUND 1:

DCM solution of the ligand (21 mg, 1mL) was taken into a glass tube onto which was poured toluene (1 ml) above which was layered methanolic solution of $Cd(ClO_4)_2$ (31 mg, 1mL). Block Shaped yellow crystals suitable for X-ray studies were obtained after 15 days in 60 % yield.

Compound 1: FT-IR (KBr pellet, cm^{-1}): 3454.64(m), 1952.58 (w), 1612.45 (s), 1549.93 (m), 1422.12 (m), 1317.68 (w), 1233.16 (s), 1100.22 (s), 813.22 (m), 728.81 (m), 683.46 (m), 620.93 (m), 513.05 (m).

Elemental analysis (%): *Calculated* for $C_{32}H_{32}CdCl_2N_8O_{17}$: C 39.02, H 3.27 and N 11.38. *Found*: C 40.15, H 3.89 and N 10.89.

SYNTHESIS OF COMPOUND 2:

DCM solution of the ligand (21 mg, 1mL) was taken into a glass tube onto which was poured mesitylene (1 ml) above which was layered methanolic solution of $Cd(ClO)_4$

(31 mg, 1mL). Block Shaped yellow crystals suitable for X-ray studies were obtained after 15 days in 60 % yield.

Compound 2: FT-IR (KBr pellet, cm^{-1}): 3460.15 (m), 1947.05 (w), 1703.16 (w), 1612.45 (s), 1556.11 (w), 1420.06 (m), 1312.18 (m), 1233.16 (m), 1103.29(s), 824.32 (m), 683.46 (m), 631.92 (m), 518.55 (m).

Elemental analysis (%): *Calculated* for $C_{76}H_{76}Cd_2Cl_4N_{16}O_{16}$: C 29.86, H 2.50 and N 7.33. *Found*: C 30.12, H 2.89 and N 6.89.

ANION EXCHANGE STUDIES:

Solid powder of compounds **1** and **2** were separately stirred very slowly in methanolic solutions (1 mmol/10 mL MeOH) of NaN_3, KSCN and $NaN(CN)_2$ for about 7 days at RT which yielded the anion exchanged product. The products were characterized by FT-IR, XPRD & diffused reflectance spectra, solid- state emission spectra.

ANION SELECTIVITY TEST:

Separation of N_3^- and SCN^- :

Solid powder of compound **1** and **2** were separately stirred very slowly in methanolic solution (10 mL) of equimolar NaN_3(1 mmol) and KSCN (1 mmol) for about 7 days at RT giving rise to the anion exchange product, characterized by FT-IR spectra.

Separation of SCN^- and $N(CN)_2^-$:

Solid powder of compound **1** and **2** were separately stirred very slowly in methanolic solution (10 mL) of equimolar KSCN(1 mmol) and $NaN(CN)_2$ (1 mmol) for about 7 days at RT giving rise to the anion exchange product, characterized by FT-IR spectra.

Separation of $N(CN)_2^-$ and N_3^-:

Solid powder of compound **1** and **2** were separately stirred very slowly in methanolic solution (10 mL) of equimolar $NaN(CN)_2$(1 mmol) and NaN_3 (1 mmol) for about 7

days at RT giving rise to the anion exchange product, characterized by FT-IR spectra.

PHYSICAL MEASUREMENTS:

- **Powder X-ray Diffraction (PXRD)**:

PXRD patterns were measured on *Bruker D8 Advanced X-Ray Diffractometer* at room temperature using Cu-Kαradiation (1.5406 Å) with a scan speed of 0.5° min^{-1} and a step size of 0.01° in 2 *theta*.

- **Thermogravimetric analysis (TGA):**

TGA was recorded on Perkin-Elmer STA 6000, TGA analyser under N_2 atmosphere with heating rate of 10°C min^{-1}.

- **Infra-Red Spectroscopy (IR):**

IR-spectra were recorded on a *Thermoscientific*–Nicolet-6700 FT-IR spectrometer. FT-IR spectra were recorded on *NICOLET 6700 FT-IR Spectrophotometer* using KBr Pellets.

- **Solid-state UV**: Solid state fluorescence was recorded on Perkin Elmer Lamda 900 UV/ VIS Spectrometer.

- **Solid-state fluorescence:**

The solid-state fluorescence spectra were recorded on *Fluorolog 3*.

X-RAY STRUCTURAL STUDIES:

Single-crystal X-ray data of compound **1** and **2** were collected at 150 K on a Bruker KAPPA APEX II CCD Duo diffractometer (operated at 1500W power: 50 kV, 30 mA) using graphite-monochromated Mo Kα radiation (λ= 0.71073 Å).Crystal was on nylon CryoLoops (Hampton Research) with Paraton-N (Hampton Research).The data integration and reduction were processed with SAINT1 software. A multi-scan absorption correction was applied to the collected reflections. The structure was solved by thedirect method using SHELXTL2 and was refined on F2 by full-matrix

least-squares technique using the SHELXL-973 program package within the WINGX4 programme. All non-hydrogen atoms were refined anisotropically. All hydrogen atoms were located in successive difference Fourier maps and they were treated as riding atoms using SHELXL default parameters. The structures were examined using the *Adsym* subroutine of PLATON5 to assure that no additional symmetry could be applied to the models.

RESULTS AND DISCUSSION

The design of the organic linker forms a pivotal part in obtaining desired properties in a metal-organic framework. Literature reviews have emphasized the importance of size and shape of the co-ordinating ligand.

CRYSTAL STRUCTURES:

➢ Compound 1:

Yellow coloured crystals of compound **1** were obtained by layering of $Cd(ClO_4)_2$ and ligand **L** in a solvent system of dichloromethane (DCM), methanol (MeOH) and toluene. Single crystal analysis revealed the formation of two-dimensional net. Single crystal X-ray diffraction (SC-XRD) analysis showed that compound **1** crystallised in a monoclinic space group P21/c. An asymmetric unit of the compound consists of an octahedral Cd(II) atom, two co-ordinated ligands, (wherein one was in trans geometry and the other showed distorted cis), two ClO_4^- ions , one

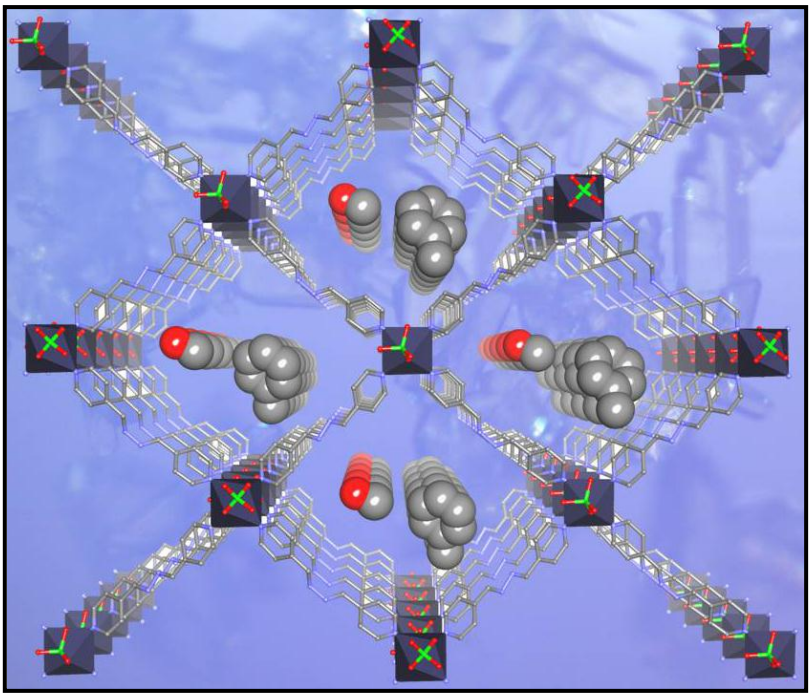

Figure 6: Perspective view of compound 1 showing similar nets

MeOH and one toluene represented by **$[\{Cd(L)_2(ClO_4)_2\}.(Toluene).(MeOH)]_n$**. Amongst the two perchlorate anions bound to the metal site, one was monodentately bound whilst the other bi-dentately. Co-ordination via terminal $N_{pyridyl}$ donors extended the structure in a zigzag fashion to form a two-dimensional net. The nets were not planar owing to the distorted cis-geometry of one of the ligands (*Figure 8*).

Guest molecules were encapsulated in the voids between the two nets. The methanol molecule formed H-bond with the oxygen of the bi-dentately bound perchlorate anion. CH-π interactions were observed between the CH of the distorted cis-ligand and the π cloud of toluene.

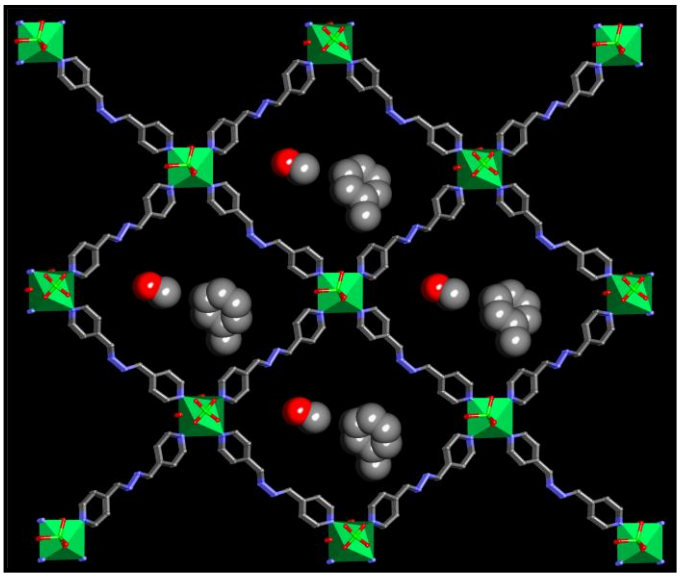

Figure 7: 2D packing of compound 1 showing free guests in the channel

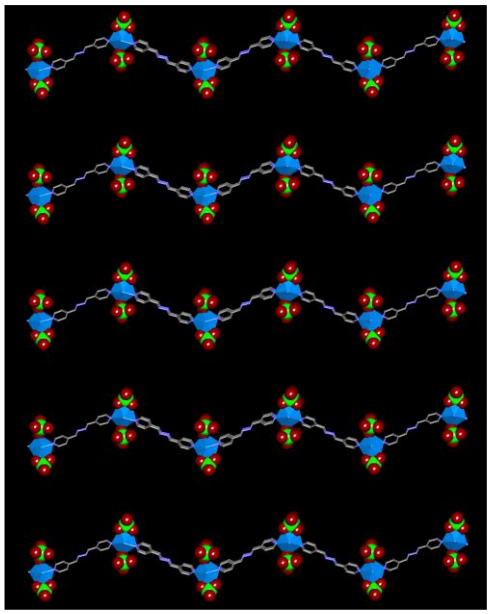

Figure 8: 2D non planar sheets of Compound 1

Table 1: Crystal data and structure refinement for Compound 1.

Identification code	Compound 1	
Empirical formula	$C_{32}H_{32}CdCl_2N_8O_{17}$	
Formula weight	983.96	
Temperature	100(2) K	
Wavelength	0.71073 Å	
Crystal system	Monoclinic	
Space group	P21/c	
Unit cell dimensions	a = 11.9813(11) Å	α= 90°.
	b = 22.629(2) Å	β= 103.465(2) °
	c = 13.4193(13) Å	γ = 90°.
Volume	3538.2(6) $Å^3$	
Z	4	
Density (calculated)	1.847 Mg/m^3	
Absorption coefficient	0.863 mm^{-1}	
F (000)	1992	
Crystal size	0.18x 0.14x 0.10 mm^3	
Theta range for data collection	1.75 to 28.31°.	
Index ranges	-15<=h<=15, -30<=k<=30, -17<=l<=17	
Reflections collected	62607	
Independent reflections	8767 [R (int) = 0.0195]	
Completeness to theta = 28.31°	99.8 %	
Refinement method	Full-matrix least-squares on F^2	
Data / restraints / parameters	8767 / 0 / 472	
Goodness-of-fit on F^2	1.866	
Final R indices [I>2sigma (I)]	R1 = 0.0435, wR2 = 0.1980	
R indices (all data)	R1 = 0.0452, wR2 = 0.2002	
Largest diff. peak and hole	1.470 and -2.080 e.$Å^{-3}$	

➢ Compound 2:

When ligand **L** was combined with $Cd(ClO_4)_2$ in a solvent system of DCM, methanol and mesitylene yellow colored crystals of compound **2** were yielded. Single crystal X-ray diffraction (SC-XRD) analysis showed that compound **2** crystallised in a triclinic space group P-1 An asymmetric unit of the compound consisted of two metal sites coordinated to four ligand molecules, four perchlorate anions and disordered mesitylene molecules denoted by $\mathbf{[\{Cd_2(L)_4(ClO_4)_4\}.xG]_n}$. One metal site was bound to two different ligands and two perchlorate anions in a monodentate fashion. The ligand coordinated to the metal centers via the terminal nitrogens thereby, extending the framework to form a 2D

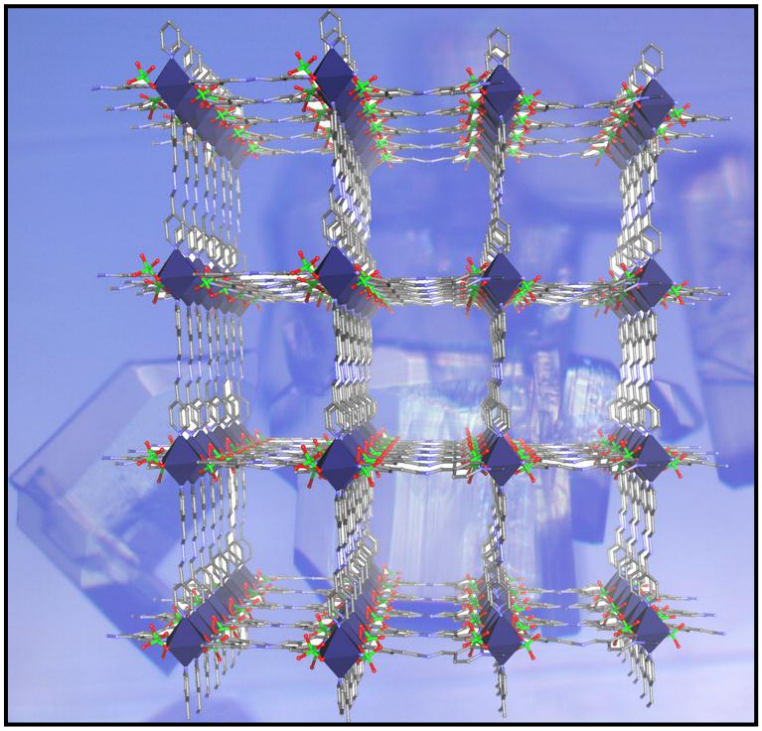

Figure 9: Perspective view of compound 2 showing similar nets

planar net (*Figure 11*). Disordered mesitylene molecules were found trapped in the interstitial positions between the nets. CH-π interactions were observed between the disordered mesitylene molecule and the pyridyl moiety.

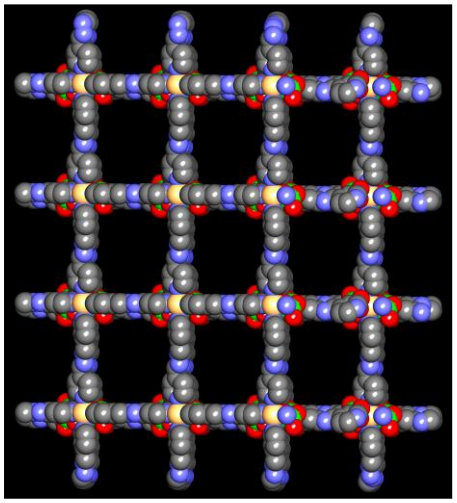

Figure 10: 2D packing of compound 2

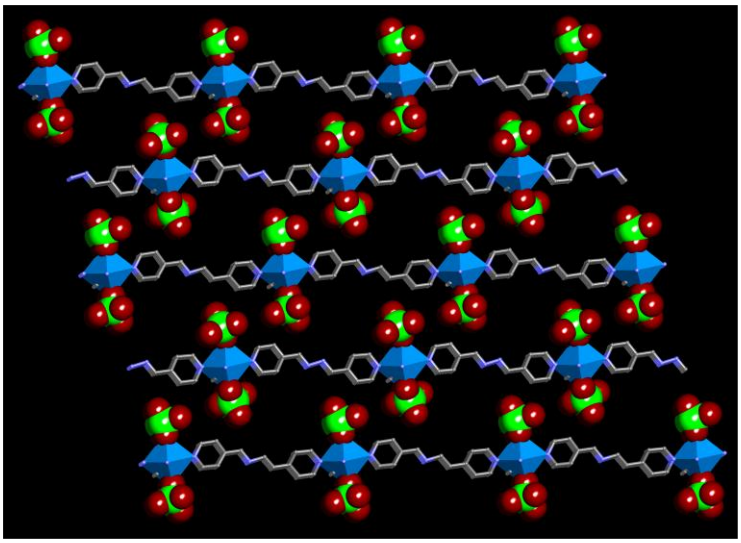

Figure 11: 2D planar sheet of compound 2

Table 2: Crystal data and structure refinement for Compound 2.

Identification code	Compound 2	
Empirical formula	$C_{76}H_{76}Cd_2C_{l4}N_{16}O_{16}$	
Formula weight	3053.41	
Temperature	100(2) K	
Wavelength	0.71073 Å	
Crystal system	Triclinic	
Space group	P-1	
Unit cell dimensions	a = 15.9116(14) Å	α= 106.406(2) °
	b = 16.0350(14) Å	β= 97.753(2) °
	c = 18.0514(16) Å	γ = 95.342(2) °
Volume	4335.9(7) $Å^3$	
Z	1	
Density (calculated)	1.169 Mg/m^3	
Absorption coefficient	0.876 mm^{-1}	
F (000)	1473	
Crystal size	0.19 x0.14 x 0.10 mm^3	
Theta range for data collection	1.19 to 28.31°.	
Index ranges	-21<=h<=20, -20<=k<=21, -24<=l<=24	
Reflections collected	75587	
Independent reflections	21430 [R (int) = 0.0324]	
Completeness to theta = 28.31°	99.3 %	
Refinement method	Full-matrix least-squares on F^2	
Data / restraints / parameters	21430 / 0 / 986	

Goodness-of-fit on F^2	3.209
Final R indices [I>2sigma (I)]	R1 = 0.1399, wR2 = 0.3970
R indices (all data)	R1 = 0.1601, wR2 = 0.4156
Largest diff. peak and hole	11.097 and -5.251 e.$Å^{-3}$

POWDER X-RAY DIFFRACTION (PXRD):

To understand the phase purity and stability of the as-synthesized compounds, powder x-ray diffraction patterns were recorded.

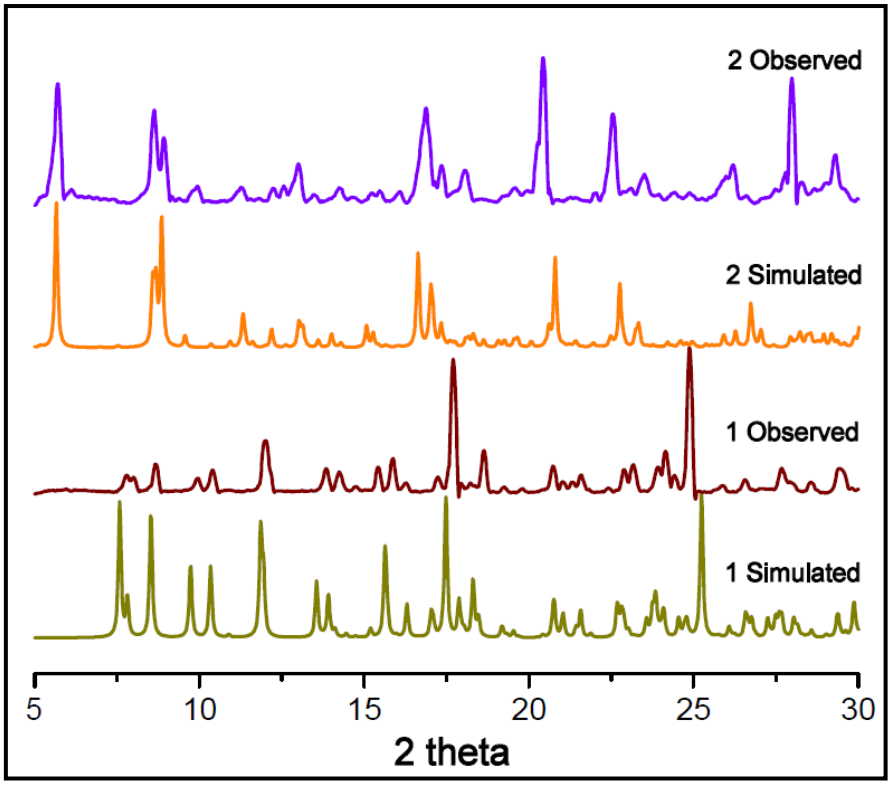

Figure 12: PXRD patterns of compound 1 and 2

PXRD patterns measured for the crystal products of complexes **1** and **2** are shown in *Figure 12*. They are in good agreement with their corresponding simulated patterns. This confirms that the single-crystal structures are representative of the bulk of the corresponding samples. Both the compounds were thus found to be pure, highly crystalline.

ANION EXCHANGE STUDIES:

Anion recognition and separation is presently a very active topic because various anions play crucial role in chemical and biological processes. The design of anion receptors, however, is challenging.

As mentioned earlier, compounds **1** and **2** had ClO_4^- anions coordinated to the metal centers. The two compounds had enough large channels available for anion access. So, we wondered if these anions could be exchanged by different kinds of anions, thus, leading to anion exchange studies. The exchange process was monitored by FT-IR spectroscopy and PXRD studies.

➢ Infra-red (IR) Studies:

When crystals of compound **1** and **2** were separately immersed in methanolic solutions of NaN_3, KSCN and $NaN(CN)_2$ respectively for seven days, the crystals of **1** and **2** underwent anion exchange. Each product was separated and characterised using FT-IR spectroscopy and PXRD measurements.

Strong bands associated with the exchanged anions were observed in each of the two cases. The disappearance of bands related to ClO_4^- validated the process. Other peaks in the spectra remained virtually unchanged, suggesting that the skeletal structure of the complexes remained intact after the exchange process. During the preservation of MOF topology and the anion-exchange process, the incoming anions occupied the same position in the crystal lattice as the displaced ClO_4^- anions. This means that the windows in **1** and **2** are large enough to facilitate movement of the incursive ions in and out of the cage.

As seen from *Figure 13* and *Figure 14*, the strong bands associated to ClO_4^- ~1100 cm^{-1} were significantly weakened, indicating that ClO_4^- in **1** and **2** was exchanged by the incursive anions, however, the exchange was not 100%, as absorption bands with diminished intensity, associated to $ClO4^-$ were observed in the anion exchanged complexes as well.

Besides, the decrease of the ClO_4^- signal, new peaks were observed in both the compounds at ~2035 cm^{-1} (characteristic of N_3^-), ~2088 cm^{-1} (characteristic of SCN^-) and ~2150 cm^{-1} (characteristic of $N(CN_2^-$) which confirmed that anion exchange reactions have occurred.

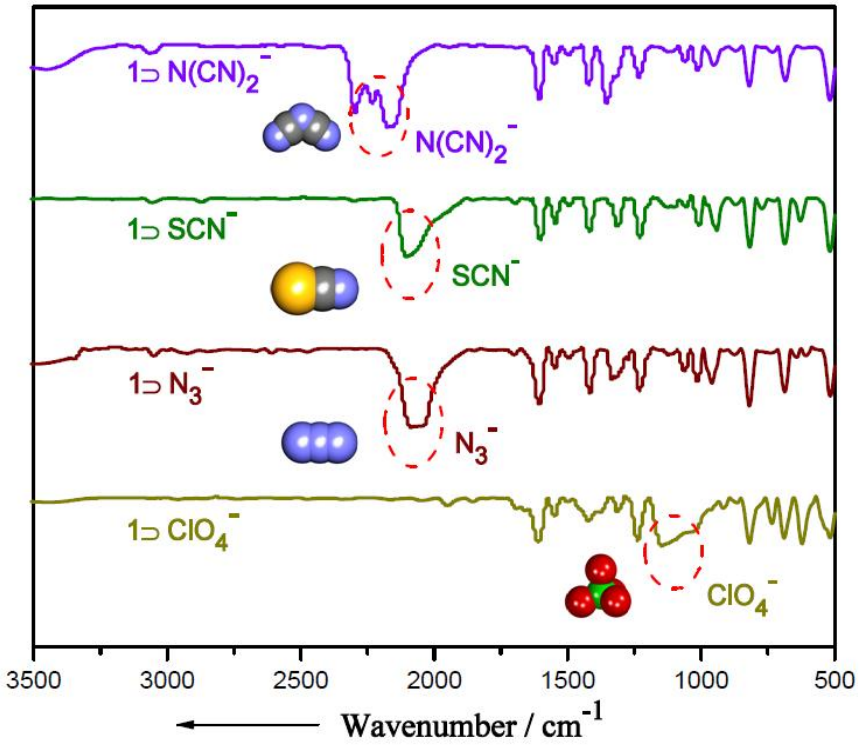

Figure 13: FT-IR spectra of Compound 1 and the anion exchanged products

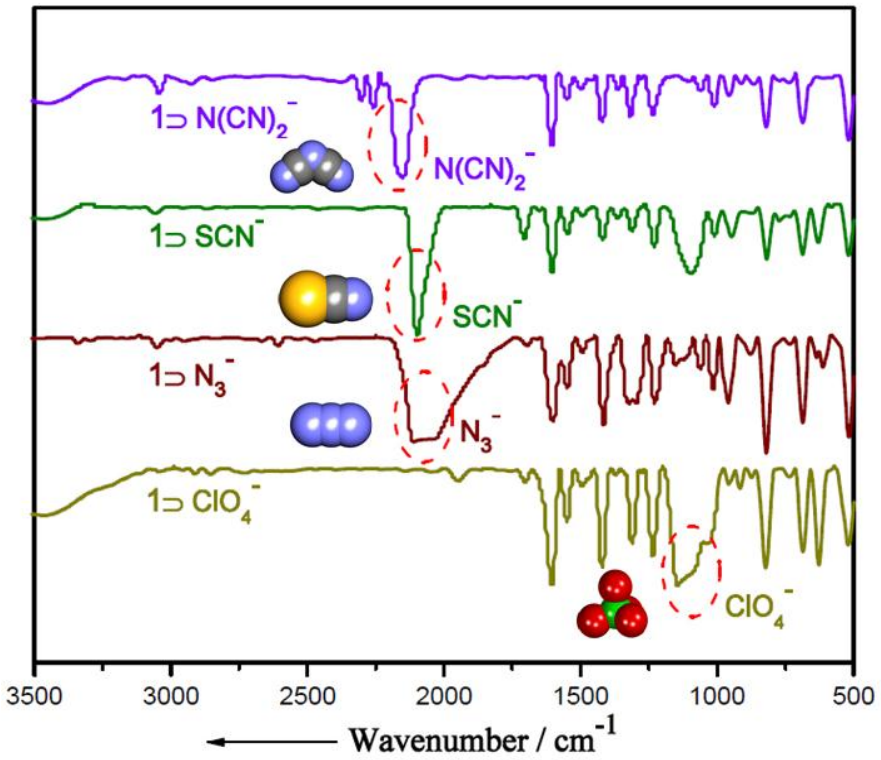

Figure 14: FT-IR spectra of Compound 2 and the anion exchanged products

➢ Powder x-ray diffraction (PXRD) studies:

In addition, the PXRD studies were conducted to the check the framework rigidity after anion exchange. The patterns measured for the anion exchanged products are shown in *Figure 15* and *Figure 16* respectively. PXRD patterns of anion-exchanged products are different for different anions because of their different shape, size, and coordinating tendency, thus showing the highly flexible nature of the framework. Thus anions playing the role of stimuli as a structure directing agent.

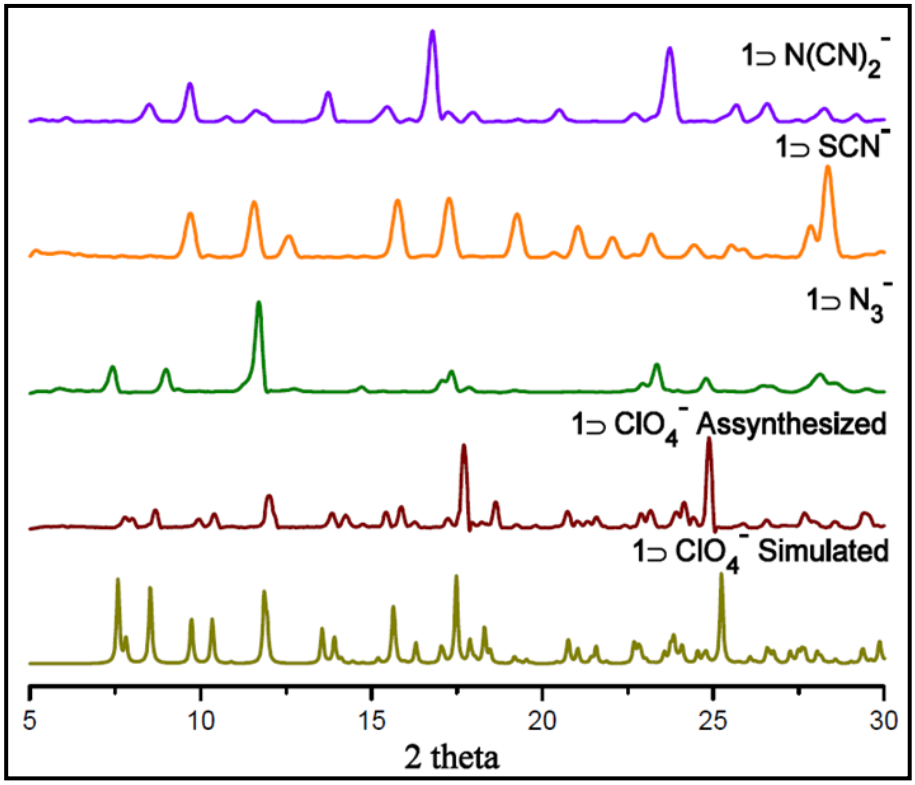

Figure 15: PXRD pattern of Compund 1 and the anion exchanged products

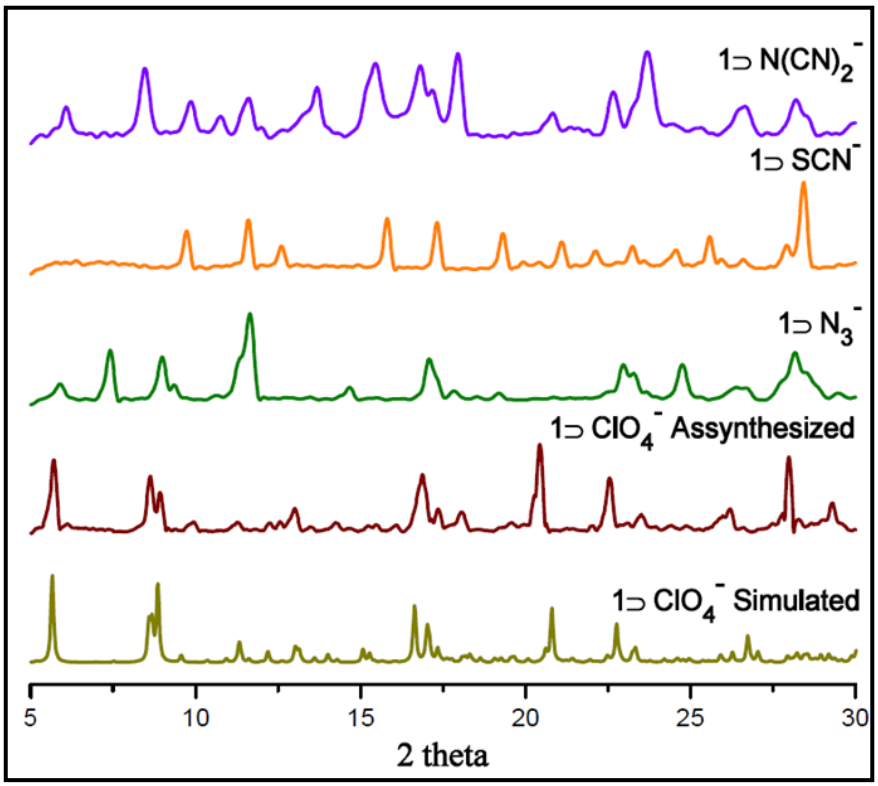

Figure 16: PXRD pattern of Compund 2 and the anion exchanged products

ANION AFFINITY TESTS:

Compared to anion-exchange, anion selectivity, i.e., capturing specific anions in the presence of other anionic competitors is more significant and challenging.

Selective anion exchange with the framework was investigated by performing anion-exchange experiments with different binary mixtures of anions. Three different binary combinations were used to study affinity, N_3^-/SCN^-, $N_3^-/N(CN)_2^-$ and $SCN^-/N(CN)_2^-$. In a typical experiment, crystals of **1** and **2** were immersed in a methanolic solution of mixed anions in equimolar concentration. Anion exchange was further monitored by FT-IR analysis to examine preferential exchange from the mixture.

All the three combinations showed selective uptake (*Figure 17* and *Figure 18*). With $N_3^-/N(CN)_2^-$, N_3^- was preferentially taken and with $SCN^-/N(CN)_2^-$, SCN^- was

selectively exchanged. However, when the experiment was conducted between N_3^- and SCN^-, N_3^- was preferred over SCN^-. Thus, the above-mentioned experiments show the order of affinity of guest anions to the framework: N_3^- > SCN^- >$N(CN)_2^-$

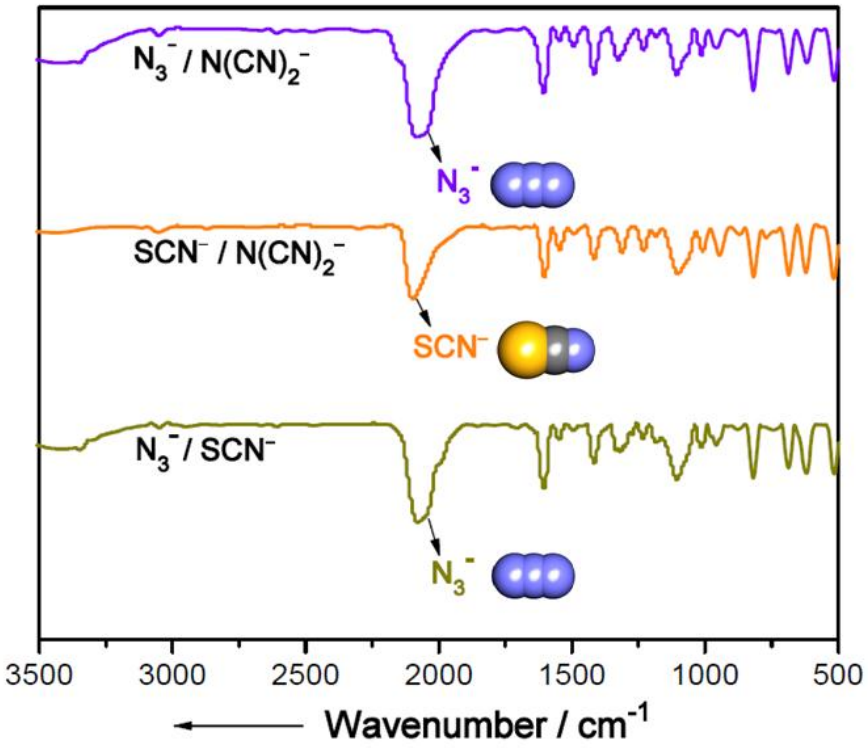

Figure 17: FT-IR spectra of the affinity test of Compound 1

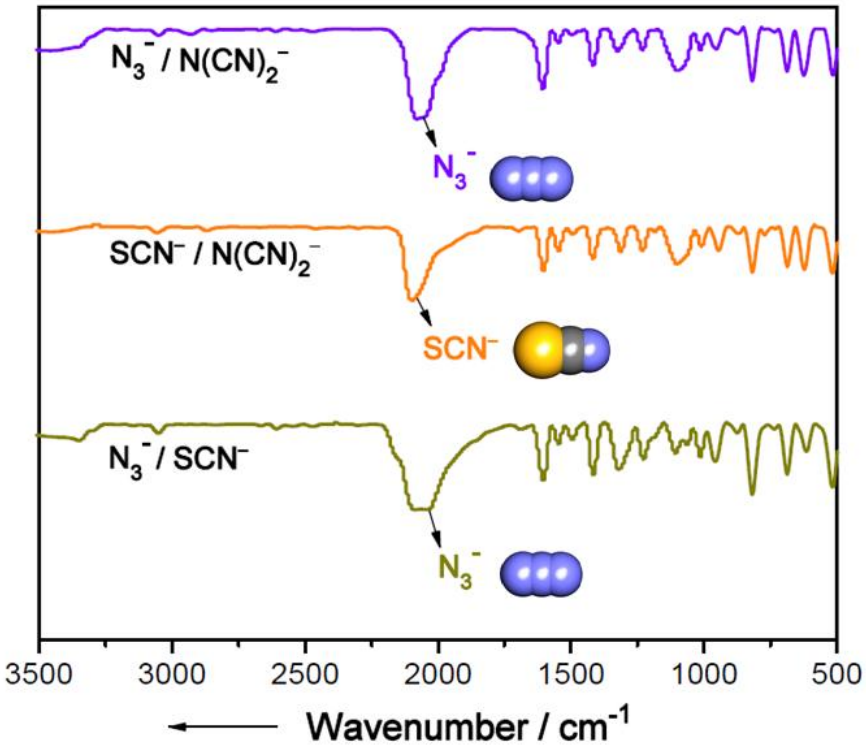

Figure 18: FT-IR spectra of the affinity test of Compound 2

These differences in affinity to the framework arise from several properties of the anions, such as their size, shape, geometry, their coordinating tendency to Cd(II), and also their different interactions with the framework. Due to weakly coordinating nature of $N(CN)_2^-$, it is going inside the framework.

THERMOGRAVIMETRIC (TGA) ANALYSIS:

The stability of compounds **1** and **2** was confirmed from TGA plots, which were conducted over temperature range of 30^0 C to 800^0 C. It was heated gradually to exclude the solvent molecules from the framework.

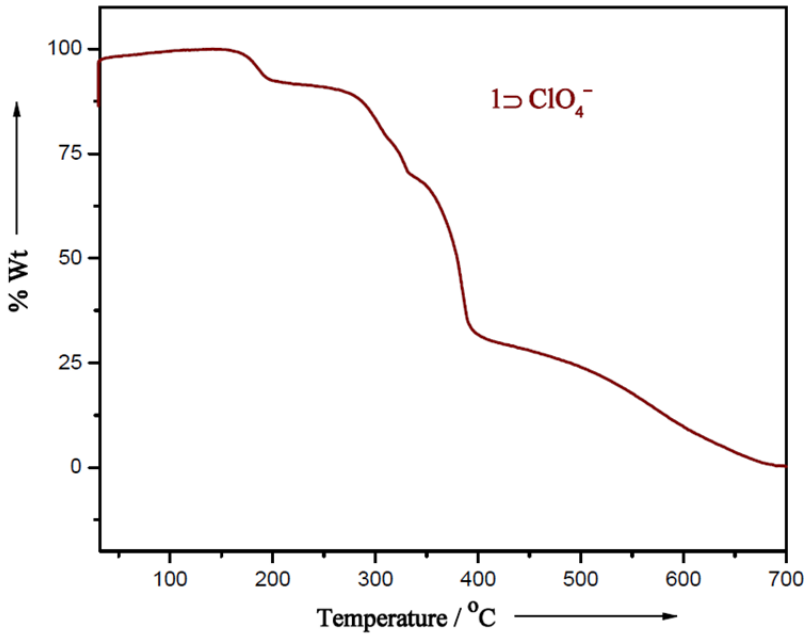

Figure 19: TGA plot of Compound 1

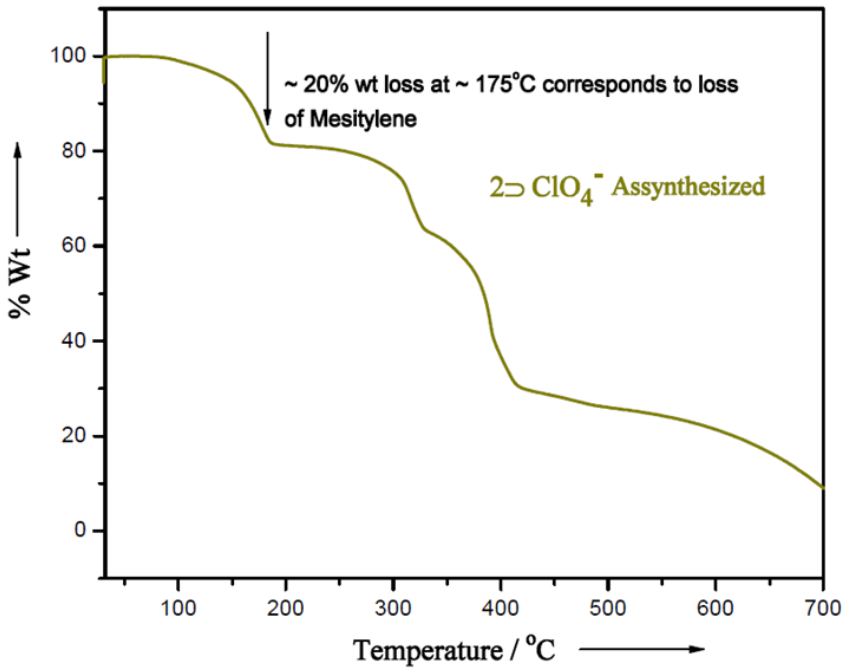

Figure 20: TGA plot of Compound 2

TGA plot of Compound **1** (*Figure 19*) showing ~ 8 % wt loss at temperature ~ 185 °C corresponding to loss of free guest molecules in the framework and further stable up to 280° C. Compound **2** (*Figure 20*) showed a 20% weight loss around 175^0 C which is consistent with the loss of mesitylene molecules and is further stable up to 300° C.

SOLID-STATE UV:

Solid-state UV absorptions were measured for **1**, **2** and all the anion-exchanged compounds to record the excitation wavelength. These absorption curves were found to be similar to that of their parent compounds. Compound **1** and its anion exchanged compounds showed minimum reflectance at wavelength ~ 355 nm (*Figure 21*). Whereas, in case of **2** and its corresponding anion exchanged products minimum reflectance was observed at wavelength ~ 355 nm (*Figure 22*).

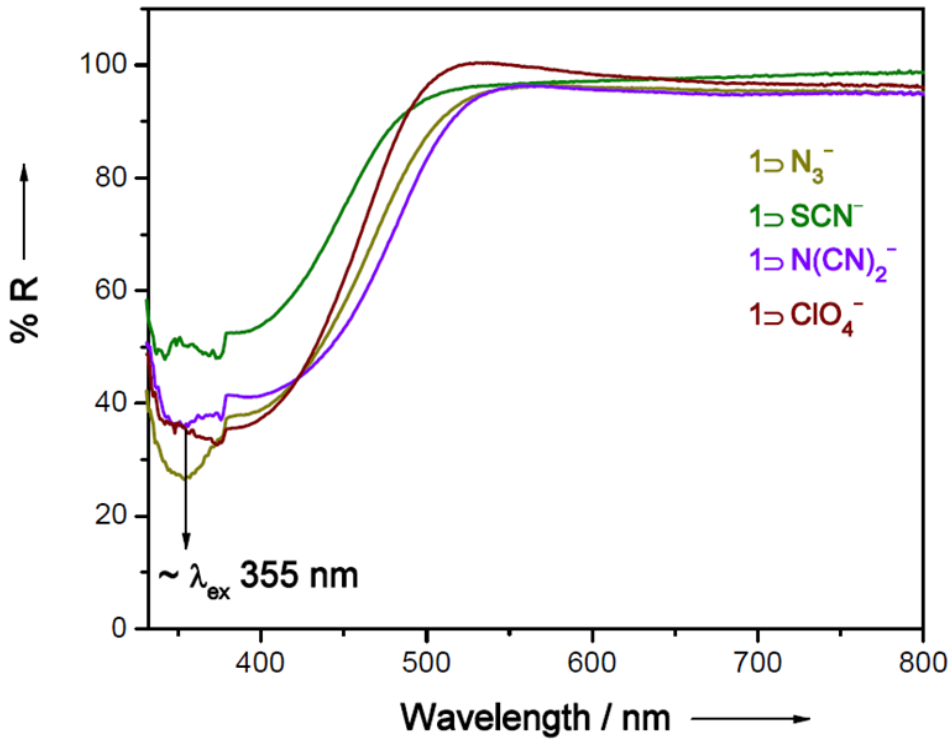

Figure 21: Solid state UV spectra of Compound 1 and anion exchanged products

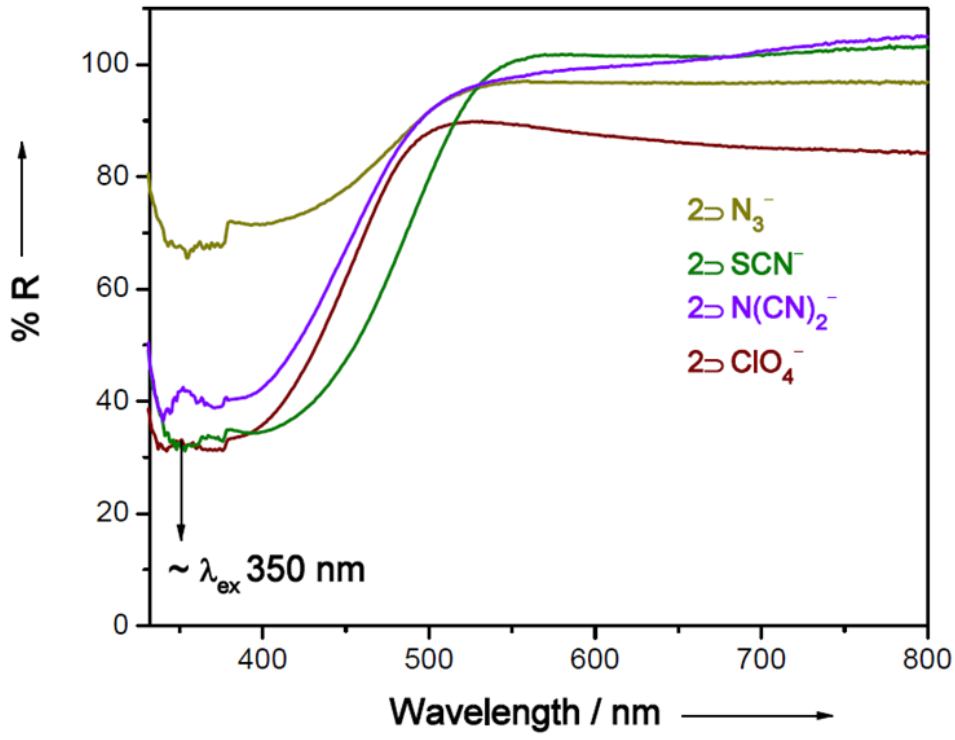

Figure 22: Solid state UV spectra of Compound 2 and anion exchanged products

FLOUROSCENCE:

Solid-state emission spectra of powder samples of the two batches which included the parent compound and the anion exchanged products were measured at room temperature.

➢ Compound 1:

Upon photo-excitation at 355 nm at room temperature, ligand **L** displayed two emission bands at 408 nm and 427 nm respectively. Compound **1** showed an emission with a maximum at around 432 nm, and a higher energy but less intense shoulder at 411 nm respectively. All the other anion exchanged products displayed emission bands with intensity maxima similar to compound **1**. (*Figure 23*) For 1⊃ $N(CN)_2^-$, the bands obtained were at around 437 nm and a less intense shoulder at 416 nm. In case of 1⊃SCN^-, intensity maxima at 436 nm and a higher energy shoulder at 415 nm were observed. However, for 1⊃N_3^-, two bands were located at 435 nm and 413 nm, the former being the intense.

The emission intensity of anion exchanged compounds was very different to the emission intensity of **1**. Highest enhancement in fluorescence was observed in case of $1\supset N(CN)_2^-$ followed by $1\supset SCN^-$, however, $1\supset N_3^-$ showed fluorescence quenching with respect to compound **1**.

π*-n or π*–π intra-ligand transitions are possible for the emissions of compound **1** and the exchanged compounds. The low-energy emissions in the region 430–440 nm are not purely from **L** itself (intraligand transition, IL). This could be tentatively assigned to a metal-to-ligand charge-transfer (MLCT) transition, possibly mixed with an IL transition. The high-energy emissions are most likely due to IL transitions.

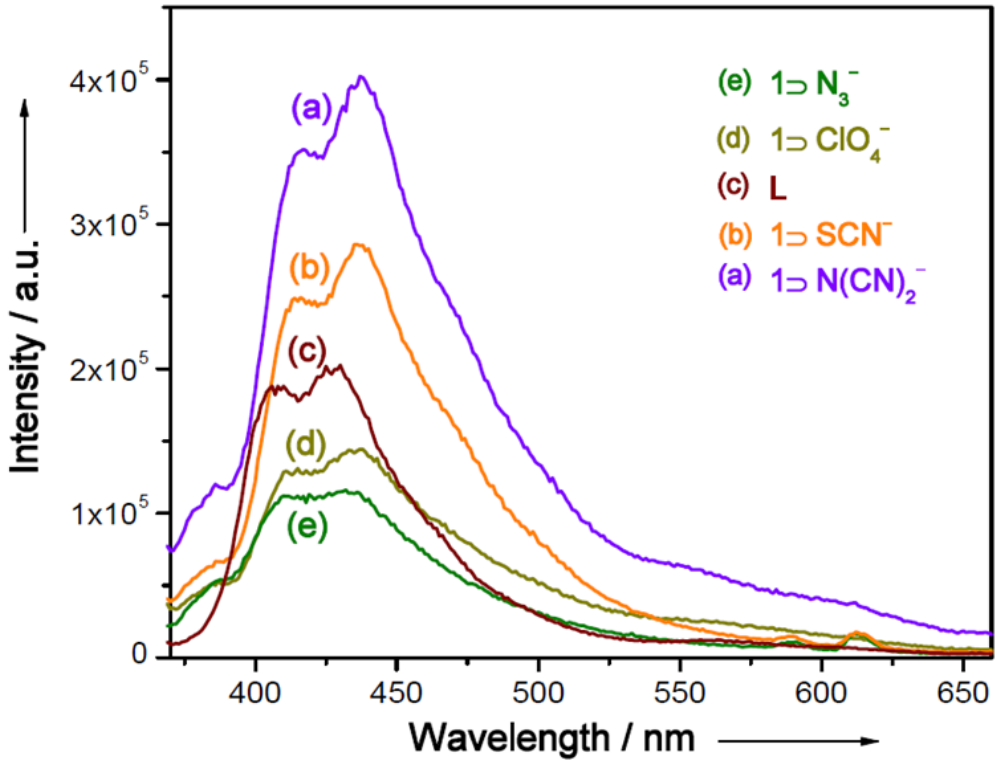

Figure 23: Solid state emission spectra of Compound 1 and anion exchanged products

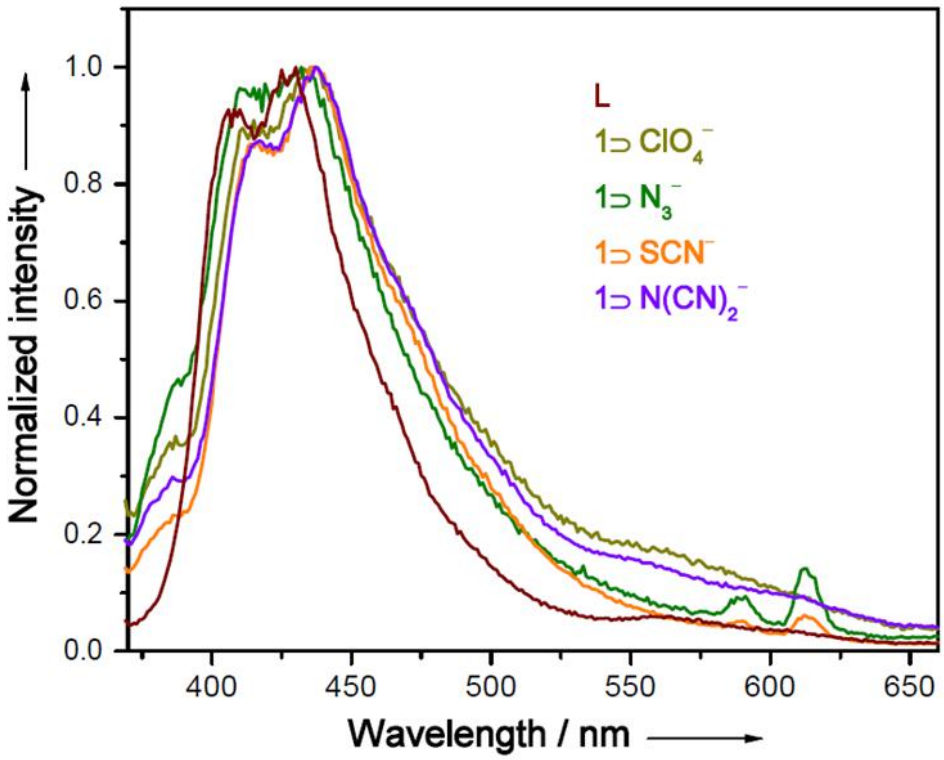

Figure 24: Normalized emission spectra of Compound 1 and anion exchanged products

➢ Compound 2:

Solid samples of **2** showed an emission profile similar to **1** upon photo-excitation at 350 nm at room temperature. (*Figure 25*) The parent compound showed two emission bands at 413 nm and 434 nm respectively. The anion exchanged compounds viz. 1⊃ $N(CN)_2^-$, 1⊃SCN^- and 1⊃N_3^- displayed emission bands with intensity maxima at 437 nm, 435 nm and 434 nm and higher energy shoulders at 417 nm, 414 nm and 412 nm respectively.

Similar to the trend observed in case of **1**, 1⊃ $N(CN)_2^-$ showed the highest intense profile, followed by 1⊃SCN^- and the least in case of 1⊃N_3^-.

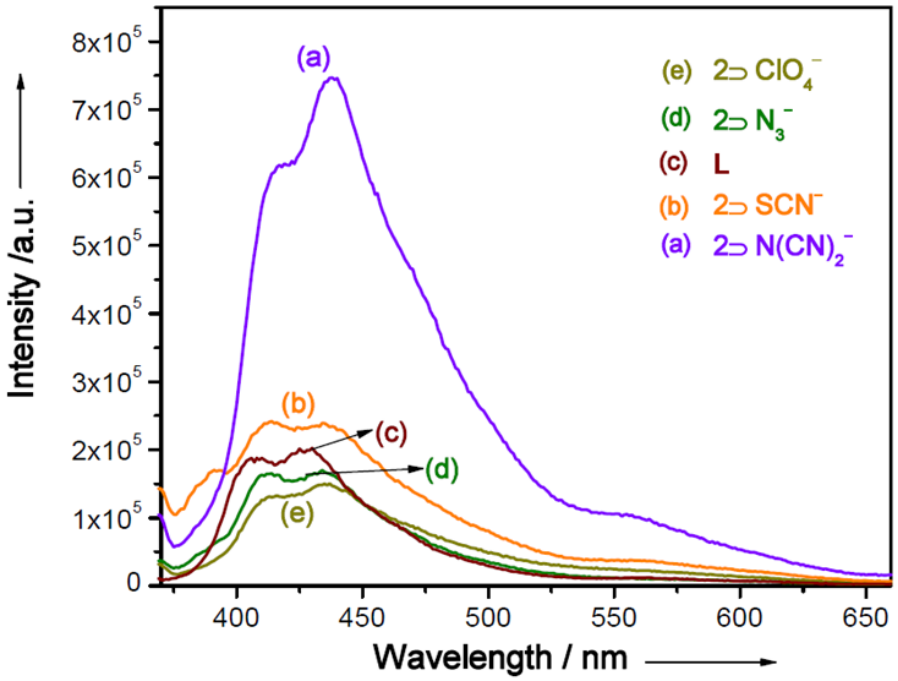

Figure 25: Solid state emission spectra of Compound 2 and anion exchanged products

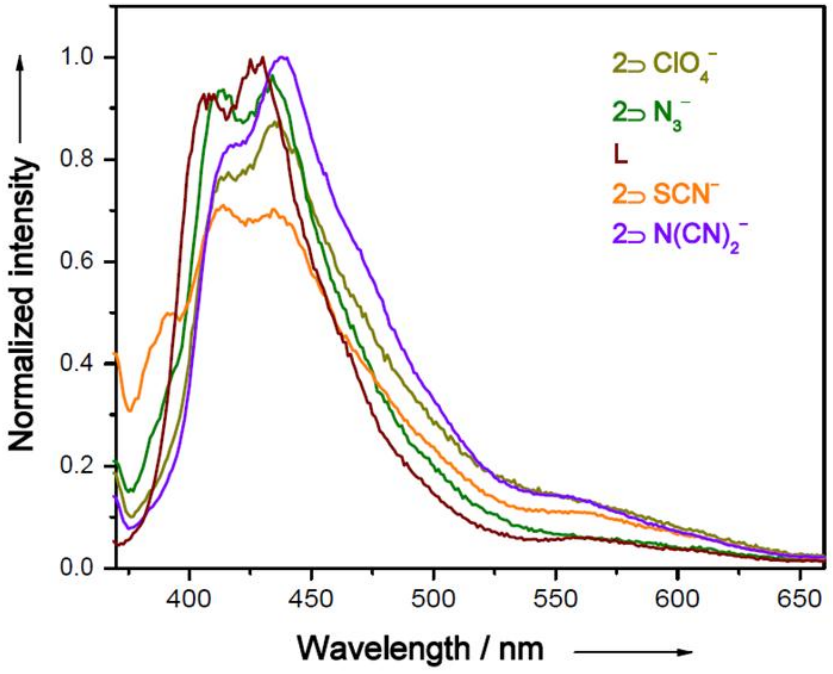

Figure 26: Normalized emission spectra of Compound 2 and anion exchanged products

The reason behind the order of observed luminescence for the different anion-exchanged compounds is not very well-known; this can be attributed to the various electronic interactions of the anions with the framework walls and the Cd(II) centre which is largely dependent on their size, geometry, and coordinating tendencies. Being a weakly coordinating in nature $N(CN)_2^-$ can easily occupy different positions within the dynamic framework after undergoing exchange reaction with ClO_4^- which can eventually increases the intra ligand (IL) interactions subsequently enhancement in luminescence occurs .On the other hand, we know that N_3^- and SCN^- are strongly coordinating anions. Therefore, there is a possibility that the coordination of these anions to the metal centre may lead to drastic structural changes within the framework. This in turn may diminish the intra ligand interactions, thus, reducing the luminescence intensities.

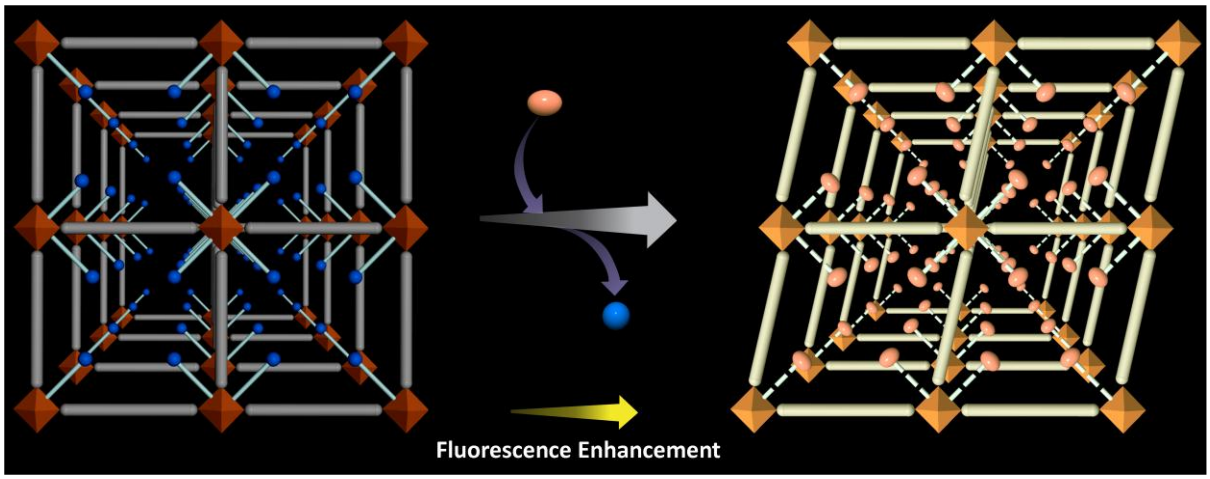

Figure 27: Schematic representation showing anion responsive structural transformation and fluorescence enhancement

CONCLUSION

In summary we used a linear bichelating N-donor ligand **L** to obtain two neutral 2D frameworks. Both the frameworks contain $ClO4^{-}$ ions which are coordinated to metal centre. These coordinated anions in both compounds can be quantitatively exchanged with other strongly coordinating (SCN^{-} and N_3^{-}) and weakly coordinated anion ($N(CN)_2^{-}$) as evidenced by the infrared absorption spectroscopy. The compounds exhibit anion dependent structural dynamic behaviour which is well demonstrated by their PXRD patterns. Moreover, the compounds showed selective anion exchange and the affinity of guest anions towards the framework N_3^{-}> SCN^{-}> $N(CN)_2^{-}$. Both the frameworks and their anion exchanged compounds display emission profiles which may be attributed to intraligand (IL) transitions mixed with MLCT. Interestingly, the emission intensities of the anion exchanged compounds are very different to the emission intensity of **1** and **2**. Weakly coordinating anions like $N(CN)_2^{-}$ showed highest enhancement in fluorescence, however, anions with higher coordinating tendency like SCN^{-} N_3^{-} and showed lesser intense emission profiles. Such anion-responsive tunable luminescent compounds may seek potential biological and industrial applications.

REFERENCES

(1). (a) Yang, R. T. *Gas Separation by Adsorption Progress*, Butterworth, Boston, **1987**. (b) Xu, R.; Pang, W.; Yu, J.; Huo, Q.; Chen, J*. Chemistry of Zeolites and Related Porous Materials: Synthesis and Structure*, John Wiley & Sons (Asia) Pet Ltd., Singapore, **2007**. (c) Paillaud, J-L.; Harbuzaru, B.; Patarin, J.; Bats,N. Extra-Large–Pore Zeolites with Two-Dimensional Channels Formed by 14 and 12 Rings. *Science.* **2004,** *304*, 990-992.

(2). (a) Yaghi,O.M.; Li, G.; Li, H. Selective binding and removal of guests in a microporous metal-organic framework. *Nature*. **1995**, *378*, 703-706. (b) Yaghi, O.M.; Li, Hailian.; Groy, T. L. Construction of Porous Solids from Hydrogen-Bonded Metal Complexes of 1,3,5-Benzenetricarboxylic acid. *J. Am. Chem. Soc.* **1996**, *118*, 9096-9101.

(3). (a) Eddaoudi, M.; Kim, J.; Rosi, N.; Vodak, D.; Wachter, J .; Õ Keeffe, Yaghi, O. M. Systematic Design of Pore Size and Functionality in Isoreticular MOFs and Their Application in Methane Storage. *Science*, **2002**, *295*, 469-472.(b Li, J-R.; Kuppler, R. J.; Zhou,H.-C. Selective gas adsorption and separation in metal–organic frameworks. *Chem. Soc. Rev.* **2009**, *38*, 1477–1504.

(4). Evans, O. R.; Lin, W. Crystal Engineering of NLO Materials Based on Metal−Organic Coordination Networks. *Acc. Chem. Res.* **2002**, *35*, 511-522.

(5). Chen, B.; Xiang, S.; Qian, G. Metal-Organic Frameworks with Functional Pores for Recognition of Small Molecules**.** *Acc.Chem.Res*. **2010**, *43*, 1115-1124.

(6). Ma, L.; Abney, C.; Lin, W. Enantioselective catalysis with homochiral metal-organic frameworks. *Chem. Soc. Rev.* **2009**, *38*, 1248–1256.

(7). Horike, S.; Shimomura, S.; Kitagawa,S. Soft porous crystals.*Nat.Chem*.**2009**,*1*, 695-704.

(8). Manna, B.; Chaudhari, A.K.; Joarder, B.; Karmakar, A.; Ghosh, S.K. Dynamic Structural Behavior and Anion-Responsive Tunable Luminescence of a Flexible Cationic Metal–Organic Framework. *Angew.Chem. Int. Ed.* **2013**, *52*, 998-1002.

(9). Maji, T. K.; Matsuda,R.; Kitagawa,S. A flexible interpenetrating coordination framework with a bimodal porous functionality. *Nat. Mater*. **2007**, *6*, 142 –148.

(10). Allendorf,M. D.; Bauer,C. A.; Bhaktaa, R. K.; Houk, R. J. T. Luminescent metal–organic frameworks. *Chem.Soc.Rev*. **2009**, *38*, 1330–1352.

(11). (a) Chen, Y.-Q.; Li, G.-R.; Chang, Z.; Qu,Y.-K.; Zhang, Y.-H.; Bu,X.-H. A Cu(I) metal-organic framework with 4-fold helical channels for sensing anions. *Chem. Sci.* **2013**,*4*, 3678-3682. (b) Li, X.; Xu, H.; Kong, F.; Wang,R. A Cationic Metal–Organic Framework Consisting of Nanoscale Cages:Capture,Separation, and Luminescent Probing of $Cr_2O_7^{2-}$ through a Single-Crystal to Single-Crystal Process. *Angew. Chem. Int. Ed*. **2013**, *52*, 13769 –13773.

(12). Takashima, Y.; Martnez, V. M.; Furukawa, S.; Kondo, M.; Shimomura, S.; Uehara, H.; Nakahama, M.; Sugimoto, K.; Kitagawa, S. Molecular decoding using luminescence from an entangled porous framework. *Nat. Commun*. **2011**, *2*, 168-175.

(13). Wang, J-H.; Li, M.; Li, D. A dynamic, luminescent and entangled MOF as a qualitative sensor for volatile organic solvents and a quantitative monitor for acetonitrile vapour. *Chem. Sci.* **2013**, *4*, 1793-1801.

(14). Subramanian, S.; Zaworotko, M. J. Porous Solids by Design: $[Zn(4,4'\text{-bpy})_2(SiF_6)]_n \cdot x$DMF, a Single Framework Octahedral Coordination Polymer with Large Square Channels Angew*. chem .Int. Ed. Engl*. **1995** , *34,* 2127-2128.

(15). Xiang, S.-C.; Zhang, Z.; Zhao, C.-G.; Hong, K.; Zhao, X.; Ding, D.-R.; Xie, M.H.; Wu, C.D.; Das, M. C.; Gill, R.; Thomas, K. M.; Chen, B. Rationally tuned micropores within enantiopure metal-organic frameworks for highly selective separation of acetylene and ethylene. *Nat. Commun.* **2011***, 2,* 204-210.

(16). Ciurtin, D. M.; Dong, Y.-B.; Smith, M. D.; Barclay, T.; Loye, H.-C. Z. Two

Versatile *N*,*N*′-Bipyridine-Type Ligands for Preparing Organic-Inorganic Coordination Polymers: New Cobalt- and Nickel-Containing Framework Materials. *Inorg. Chem.* **2001,** *40,* 2825-2834.